Biophysical Chemistry 11 (1980) 249–255

DETERMINATION OF LIGAND-BINDING CONSTANTS BY ISOELECTRIC FOCUSING. GENERALIZATION AND EXTENSION OF THEORY *,+

John R. CANN
Department of Biophysics and Genetics, University of Colorado Health Sciences Center, Denver, Colorado 80262, USA

Received 30 October 1979

The theory of a proposed isoelectric focusing procedure for the determination of ligand binding constants has been generalized (via numerical calculations) to non-linear, electrophoretic velocity profiles and systems for which the change in velocity of the protein accompanying ligand binding depends upon pH. The theory has also been extended to include binding of ligand to heterogeneous sites. Determination of accurate values of the binding parameters depends upon extrapolation of apparent parameters to infinite dilution of protein.

1. Introduction

Recently [1] a theory has been formulated for a proposed isoelectric focusing procedure which permits determination of the intrinsic binding constant, K_0, for statistical binding of a charged ligand, $\mathcal{L}$, to ν equivalent sites on a protein molecule, $\mathcal{P}$. The protein is first focused in the absence of ligand, taking up position x_0 in the focusing column, after which ligand is added to the appropriate electrode compartment and then driven by the electric field into the column where it complexes with the protein. The band of $\mathcal{P}$ and its complexes, $\mathcal{P}\mathcal{L}_i$, migrates to a new position, $\bar{x}$, corresponding to the constituent isoelectric point of the protein in the equilibrium mixture. The reciprocal of the overall distance moved is linearly related to the reciprocal of the local concentration of the free ligand, $C_{\mathcal{L}}(\bar{x})$, by the equation

$$\frac{1}{(\bar{x}-x_0)} = \frac{1}{(x_f-x_0)} + \frac{1}{(x_f-x_0)} \cdot \frac{1}{K_0} \cdot \frac{1}{C_{\mathcal{L}}(\bar{x})}, \qquad (1)$$

where x_f is the position of the isoelectric point of the fully liganded protein.

An experimental design for application of eq. (1) involves determination of $\bar{x}$ for differing concentration of ligand added to the electrode compartment. The value of K_0 is given by the quotient of the intercept and slope of the plot of $1/(\bar{x}-x_0)$ against $1/C_{\mathcal{L}}(\bar{x})$. Since $C_{\mathcal{L}}(\bar{x})$ would be difficult to determine, it has been proposed that the concentration of ligand in the electrode compartment, or in a cross-sectional segment of the column between the focused zone of constituent protein and the electrode compartment, be used instead. Under this approximation an apparent binding constant, K_{app}, is obtained, although for certain systems conditions may be realized which give a K_{app} within 4% of K_0. In all cases, extrapolation of K_{app} to infinite dilution of protein yields K_0. The reason for this behavior is that, at finite protein concentration, the steady-state distribution of free ligand along the focusing column is not uniform throughout, showing a trough at the position of the focused peak of constituent protein. As the protein concentration is decreased, the trough decreases in depth finally disappearing in the limit of infinite dilution.

Derivation of eq. (1) makes the assumptions that (1) the electrophoretic velocity of $\mathcal{P}$ is a linear function of position in the isoelectric focusing column and

* Supported in part by Research Grant 5RO1 HL 13909-28 from the National Heart, Lung and Blood Institute, National Institutes of Health, U.S. Public Health Service. This publication is No. 733 from the Department of Biophysics and Genetics, University of Colorado Health Sciences Center, Denver, Colorado 80262.
+ The author thanks Mr. Donald I. Stimpson for many helpful discussions during the course of this investigation.

(2) the amount, ω, by which each bound ligand molecule increases the velocity of its complex is independent of PH, i.e., the linear velocity profiles of $\mathcal{P}$ and $\mathcal{P}\mathcal{L}_i$ are parallel. While these are reasonable assumptions for most systems, in some cases the isoelectric points of $\mathcal{P}$ and $\mathcal{P}\mathcal{L}_i$ may be so different that the shape of the velocity profiles resembles a titration curve [2,3]. Also, binding of ligand might change the pK's of certain ionizable groups on the protein such that the velocity profiles are not parallel. Accordingly, our previous [1] transport calculations for isoelectric focusing, which simulate the proposed procedure and converge to the steady state, have now been extended to include non-linear and non-parallel velocity profiles with the objective of generalizing the applicability of eq. (1). The calculations are for the reaction

$$\mathcal{P} + \mathcal{L} \rightleftarrows \mathcal{P}\mathcal{L}, K_0 \qquad \text{(I)}$$

in which the protein binds a single molecule of a negatively charged ligand.

In addition, an equation analogous to eq. (1) is presented for binding of ligand to a population of non-equivalent, non-interacting sites and tested numerically by transport calculations on the heuristic two-site system.

$$\mathcal{P} + \mathcal{L} \rightleftarrows \mathcal{P}\mathcal{L}, K_1$$

$$\mathcal{P}\mathcal{L} + \mathcal{L} \rightleftarrows \mathcal{P}\mathcal{L}_2, K_2 \qquad \text{(II)}$$

Here we are concerned with procedures, not only for determination of an average binding constant, but more importantly for accurate determination of an index of the extent of heterogeneity of the sites.

2. Theory

2.1. Non-linear velocity profiles (reaction I)

The calculations are for an isoelectric focusing column 1.5 cm in length with the isoelectric point of $\mathcal{P}\mathcal{L}$ ($\mathrm{pI}_{\mathcal{P}\mathcal{L}}$) located anodically to $\mathrm{pI}_{\mathcal{P}}$. Three cases have been considered:

Case I. The electrophoretic velocities of $\mathcal{P}$ and $\mathcal{P}\mathcal{L}$ as functions of position in the focusing column are given by

$$V_{\mathcal{P}}(x) = \frac{V_{\mathcal{P}}(0)}{\tanh x_0} \tanh (x_0 - x), \qquad (2)$$

and

$$V_{\mathcal{P}\mathcal{L}}(x) = V_{\mathcal{P}}(x) - V_{\mathcal{P}}(x_f), \qquad (3)$$

in which $V_{\mathcal{P}}(0) = 1.085 \times 10^{-4}$ cm s^{-1} and $x_0 = 1.085$ cm; $V_{\mathcal{P}}(x_f) = 8.0723 \times 10^{-5}$ cm s^{-1} and $x_f = 0.405$ cm. Since $V_{\mathcal{P}}(x_f) = \omega$ is independent of position and, thus, of pH, the velocity profiles are parallel.

Case II. The velocity profile of $\mathcal{P}$ is given by eq. (2) and that of $\mathcal{P}\mathcal{L}$ by

$$V_{\mathcal{P}\mathcal{L}}(x) = S[V_{\mathcal{P}}(x) - V_{\mathcal{P}}(x_f)], \qquad (4)$$

in which the scaling factor, S, is

$$S = \left| \frac{V_{\mathcal{P}}(0)}{V_{\mathcal{P}}(1.5) - V_{\mathcal{P}}(x_f)} \right|, \qquad (5)$$

where $V_{\mathcal{P}}(1.5) = -5.35932 \times 10^{-5}$ cm s^{-1}. In this case the profiles are not parallel, ω increasing with decreasing x (i.e., with decreasing pH).

Case III. $V_{\mathcal{P}}(x)$ is given by the product of S and the right hand side of eq. (2) and $V_{\mathcal{P}\mathcal{L}}(x)$ by eqs. (2) and (3). Here ω decreases with decreasing x, so that the profiles are non-parallel in the opposite sense to Case II.

Steady-state isoelectric focusing patterns for Cases I and II were computed by following the convergence with time of the numerical solution of the simultaneous transport equations and mass action expression. In order to minimize the amount of computer time, the calculations were made for the limit of infinite dilution of protein. The limit was simulated by applying a sufficiently small amount of protein to the focusing column and maintaining the concentration of ligand, C, along the column constant in position and time [1]. This expediency reduces Reaction I to a simple isomerization with equilibrium constant, $K_0 C$, while at the same time giving physically meaningful steady-state patterns for our systems. Otherwise, the calculations are virtually the same as those described previously for linear velocity profiles [1] including the criteria for convergence to the steady-state. Steady-state isoelectric focusing patterns and values of $\bar{x}$ were computed for $K_0 = 5 \times 10^4 \mathrm{M}^{-1}$ and a range of values of C. The value of $\bar{x}$ is taken to be the mean position of the peak

of constituent protein in the steady-state pattern. The diffusion coefficients of $\mathcal{P}$ and $\mathcal{PL}$ were assigned the same value: $D = 7 \times 10^{-7}$ cm^2 s^{-1} in Case I, 6×10^{-7} cm^2 s^{-1} in Case II.

The transport calculation were dispensed with in Case III, values of $C_{\mathcal{L}}(\bar{x})$ corresponding to given values of $\bar{x}$ being calculated as follows: The constituent velocity of the protein, $\bar{V}(x)$, is given by

$$\bar{V}(x) = \alpha_{\mathcal{P}}(x)\, V_{\mathcal{P}}(x) + [1-\alpha_{\mathcal{P}}(x)]\, V_{\mathcal{PL}}(x), \qquad (6)$$

where $\alpha_{\mathcal{P}}(x)$ is the fraction of $\mathcal{P}$ in the equilibrium mixture. At $\bar{x}$, $\bar{V}(\bar{x}) = 0$ so that

$$\alpha_{\mathcal{P}}(\bar{x}) = \frac{V_{\mathcal{PL}}(\bar{x})}{V_{\mathcal{PL}}(\bar{x}) - V_{\mathcal{P}}(\bar{x})}. \qquad (7)$$

The local concentration of free ligand is related to $\alpha_{\mathcal{P}}(\bar{x})$ through the mass action expression

$$C_{\mathcal{L}}(\bar{x}) = \left[\frac{1-\alpha_{\mathcal{P}}(\bar{x})}{\alpha_{\mathcal{P}}(\bar{x})}\right]\frac{1}{K_0}. \qquad (8)$$

2.2. Binding to non-equivalent, non-interacting sites (Reaction II)

One approach to the analysis of the binding of ligand to a population of non-equivalent, non-interacting sites on a protein is to assume a continuous distribution of sites with respect to the free energy of binding [4,5]. A Sips distribution is often used [4—9] in which case the binding isotherm is

$$\bar{r} = n(\bar{K}C_{\mathcal{L}})^{\alpha}/[1+(\bar{K}C_{\mathcal{L}})^{\alpha}], \qquad 0<\alpha<1 \qquad (9)$$

where $\bar{r}$ is the number of moles of $\mathcal{L}$ bound per mole of total protein; $C_{\mathcal{L}}$ is the equilibrium concentration of free ligand; $\bar{K}$ is an average binding constant, which is equal to the reciprocal of $C_{\mathcal{L}}$ when $\bar{r} = n/2$; and α is the Sips index of heterogeneity, which is a measure of the broadness of the distribution. Eq. (9) is adapted to the proposed isoelectric focusing procedure for measuring binding constants by using it in place of the Langmuir isotherm, eq. (2) of Cann and Gardiner [1] in their derivation of eq. (1) of this paper for statistical binding to equivalent sites. This gives the analogous double-reciprocal relationship

$$\frac{1}{(\bar{x}-x_0)} = \frac{1}{(x_f-x_0)} + \frac{1}{(x_f-x_0)}\cdot\frac{1}{[\bar{K}C_{\mathcal{L}}(\bar{x})]^{\alpha}} \qquad (10)$$

for binding to heterogeneous sites.

Here too it is proposed that, in practice, the initial concentration of ligand, C, in the electrode compartment, or its concentration in a segment of the column between the focused zone of constituent protein and the compartment, be used in lieu of $C_{\mathcal{L}}(\bar{x})$. Numerical transport calculations have been made to evaluate the conditions under which this approximation can give accurate values of $\bar{K}$ and α. We proceed by making the heuristic assumption that the binding characteristics of the heterogeneous, two-site system, Reaction Set II, can be represented formally by a Sips distribution. Eqs. (9) and (10) are recast, setting $C_{\mathcal{L}} = C_{\mathcal{L}}(\bar{x}) = C$, to give

$$\log[n/\bar{r} - 1] = \alpha \log 1/\bar{K} - \alpha \log C \qquad (11)$$

and

$$\log\left[\frac{x_f-x_0}{\bar{x}-x_0} - 1\right] = \alpha \log 1/\bar{K} - \alpha \log C \qquad (12)$$

respectively. A Sips plot of $\log[n/\bar{r}-1]$ versus $\log C$ is then constructed in accordance with eq. (11), the value of $\bar{r}$ being calculated for a range of values of C using the two term isotherm

$$\bar{r} = K_1 C/(1+K_1 C) + K_2 C/(1+K_2 C), \qquad (13)$$

with $K_1 = 4 \times 10^5$ M^{-1} and $K_2 = 4 \times 10^4$ M^{-1}. The linear least-squares fit of the mid-portion of the Sips plot gives $\bar{K} = 1.26 \times 10^5$ M^{-1} and $\alpha = 0.748$. Steady-state isoelectric focusing patterns and values of $\bar{x}$ are now computed for a range of values of C and constituent protein concentration; $\log[(x_f-x_0)/(\bar{x}-x_0)-1]$ is plotted against $\log C$ in accordance with eq. (12); and apparent values of the average binding constant and index of heterogeneity, $\bar{K}_{app}$ and α_{app} respectively, are obtained by least-squares fitting of the linear mid-portion of the plot for comparison with the foregoing values of $\bar{K}$ and α.

Transient and steady-state isoelectric focusing patterns were computed for finite protein concentrations as described previously [1] except for (1) the transport of four instead of three species and (2) the use of the appropriate mass action expressions for recalculation of chemical equilibrium after each time cycle of diffusion and driven transport. As before, the protein sample load is expressed as the maximum concentration, $C^0_{\mathcal{P}}$, in the initial Gaussian distribution of $\mathcal{P}$ about its pI in the focusing column. The diffusion coefficients of $\mathcal{P}$, $\mathcal{PL}$ and $\mathcal{PL}_2$ were assigned the same

value, 6×10^{-7} cm^2 s^{-1}. The linear velocity profiles of the protein species are given by $V_i(x) = 10^{-4} \times (a_i - x)$, in which a_i is the position of the pI of species i; $a_i = 1.085$ cm for $\mathcal{P}$, 0.745 cm for $\mathcal{PL}$ and 0.405 for $\mathcal{PL}_2$. For the ligand, $D_{\mathcal{L}} = 1 \times 10^{-5}$ cm^2 s^{-1} and $V_{\mathcal{L}} = -5 \times 10^{-4}$ cm s^{-1}. The numerical procedures were checked by control calculate made for statistical binding to two equivalent sites, Reaction II with $K_1 = 2k_0, K_2 = (1/2)k_0$ and $k_0 = 5 \times 10^4$ M^{-1}.

2.3. Display of isoelectric focusing patterns

The computed isoelectric focusing patterns are displayed as plots of molar constituent concentration of protein, $\bar{C}$, against x with the anode to the left. For Reaction I, $\bar{C}$ is the sum of the concentrations of $\mathcal{P}$ and $\mathcal{PL}$; for Reaction II, $\mathcal{P}$, $\mathcal{PL}$ and $\mathcal{PL}_2$. Vertical arrows locate the isoelectric points of designated species. Representative steady-state distributions of free ligand along the focusing column are also presented for Reaction II, for which the calculations were made at finite protein concentrations.

3. Results

3.1. Non-linear velocity profiles (Reaction I)

The non-linear velocity profiles are presented in fig. 1A, and representative steady-state isoelectric focusing patterns in fig. 1B. The patterns were computed for Case I in the limit of infinite dilution of protein, the parallel velocity profiles of $\mathcal{PL}$ and $\mathcal{P}$ being given by curves a and b in fig. 1A, respectively. A fundamental feature of the patterns is the dependence of the width of the focused peak upon its position in the column. This is so because the variance of the peak about its mean is given by [10], $\sigma^2 = D/\{d\bar{V}(x)/dx)_{\bar{x}}\}$, where the value of the constituent velocity gradient at $\bar{x}$, $(d\bar{V}(x)/dx)_{\bar{x}}$, varies along the column. In the absence of ligand (pattern a in fig. 1B) the protein focuses at $pI_{\mathcal{P}}$ at which position $(d\bar{V}(x)/dx)_{\bar{x}} = (dV_{\mathcal{P}}(x)/dx)_{x_0} = 1.365 \times 10^{-4}$ s^{-1} so that $\sigma^2 = 5.128 \times 10^{-3}$ cm^2, while the almost fully liganded (99.8%) protein (pattern c) focuses at a position very close to $pI_{\mathcal{PL}}$ where $(d\bar{V}(x)/dx)_{\bar{x}} = 8.872 \times 10^{-5}$ s^{-1} and $\sigma^2 = 7.890 \times 10^{-3}$ cm^2. Thus, the peak is 24% broader at a nearly saturating concentration of ligand than in its absence. An intermediate width is shown for half-saturating concentration (pattern b), $(d\bar{V}(x)/dx)_{\bar{x}} = 1.242 \times 10^{-4}$ s^{-1} and $\sigma^2 = 5.636 \times 10^{-3}$ cm^2.

Actually, the peak for half-saturating concentration of ligand is not focused exactly between $pI_{\mathcal{P}}$ and $pI_{\mathcal{PL}}$ because $|V_{\mathcal{P}}| \neq |V_{\mathcal{PL}}|$ at that position, 0.745 cm; rather it is positioned upstream at $\bar{x} = 0.778$ cm very close to 0.780 cm where $|V_{\mathcal{P}}| = |V_{\mathcal{PL}}|$. (Not precisely at 0.780 cm because of very slight skewing.) In fact, for all values of C, $\bar{x}$ is displaced somewhat from the position that would obtain in the event of linear velocity profiles. Nevertheless, the plot of $1/(\bar{x} - x_0)$ against $1/C$ is linear (fig. 2); and the quotient of its intercept and slope gives an apparent binding constant, $K_{app} = (4.38 \pm 0.037) \times 10^4$ M^{-1}, which deviates by only 12% from the actual constant, $K_0 = 5 \times 10^4$ M^{-1}. As shown in fig. 2, the plot is also linear for Case II (curves c and b in fig. 1A for the non-paral-

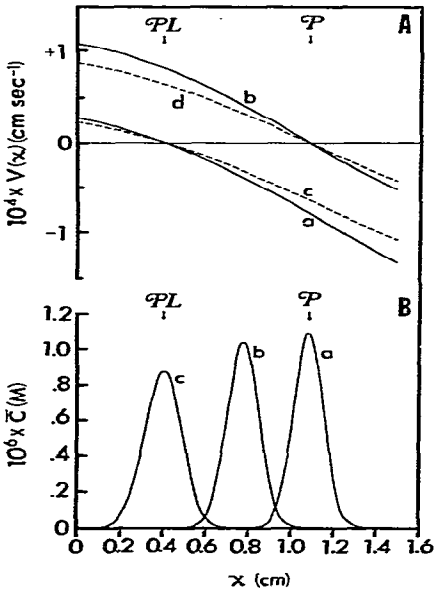

Fig. 1. Theoretical isoelectric focusing patterns (Reaction I with $K_0 = 5 \times 10^4$ M^{-1} and $C^0_{\mathcal{P}} = 1 \times 10^{-6}$ M). A. Non-linear velocity profiles used to compute the focusing characteristics in the limit of infinite dilution of protein: curves a and c, $V_{\mathcal{PL}}(x)$; b and d, $V_{\mathcal{P}}(x)$. Case I, curves a and b; Case II, c and b; Case III, a and d. B. Representative steady-state isoelectric focusing patterns computed for Case I: a, C=0; b, 2×10^{-5} M; c, 1×10^{-2} M.

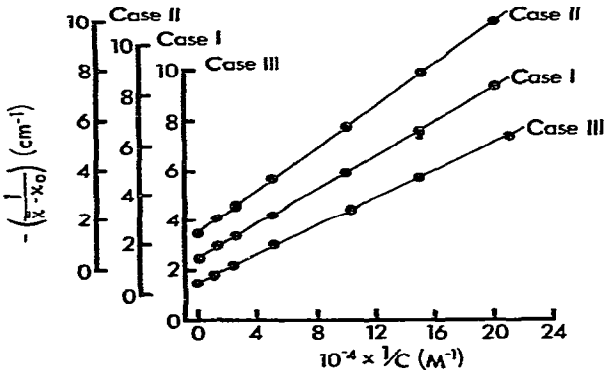

Fig. 2. Double reciprocal plot of steady-state isoelectric focusing data simulated numerically for Reaction I ($K_0 = 5 \times 10^4$ M^{-1}) in the limit of infinite dilution of protein. The straight lines are the least-squares fits: Case I, $(\bar{x}-x_0)^{-1} = -(1.508 \pm 0.0019) - (3.443 \pm 0.0114) \times 10^{-5} C^{-1}$ with standard error of estimate, $\sigma_y = 2.66 \times 10^{-2}$ cm^{-1}; Case II, $(\bar{x}-x_0)^{-1} = -(1.515 \pm 0.0133) - (4.247 \pm 0.0128) \times 10^{-5} C^{-1}$, $\sigma_y = 2.29 \times 10^{-2}$ cm^{-1}; Case III, $(\bar{x}-x_0)^{-1} = -(1.511 \pm 0.0104) - (2.806 \pm 0.0097) \times 10^{-5} C^{-1}$, $\sigma_y = 2.34 \times 10^{-2}$ cm^{-1}.

lel velocity profiles of $\mathcal{PL}$ and $\mathcal{P}$, respectively) and Case III (curves a and d). In Case II, $K_{app} = (3.57 \pm 0.033) \times 10^4$ M^{-1} which deviates by 29% from K_0; Case III, $K_{app} = (5.39 \pm 0.041) \times 10^4$ M^{-1} or 8% derivation from K_0.

These results are for a negatively charged ligand. For a positive ligand, $\text{pI}_{\mathcal{P}} < \text{pI}_{\mathcal{PL}}$; the velocity profiles are interchanged; and the values of K_{app} deviate from K_0 by the same percentages as for a negative ligand but in the opposite sense.

3.2. Binding to non-equivalent, non-interacting sites (Reaction II)

The velocity profiles of $\mathcal{P}$, $\mathcal{PL}$ and $\mathcal{PL}_2$ are presented in fig. 3A. The abscissal coordinate is the same as in our previously reported calculations [1] for binding to a single site, Reaction I with $K_0 = 5 \times 10^4$ M^{-1}; the linear velocity profiles of $\mathcal{P}$ and $\mathcal{PL}_2$ are the same as previously assigned to $\mathcal{P}$ and $\mathcal{PL}$; $\text{pI}_{\mathcal{PL}}$ is positioned exactly midway between $\text{pI}_{\mathcal{P}}$ and $\text{pI}_{\mathcal{PL}_2}$; and ω is a constant. Accordingly, it was anticipated that the control calculations on statistical binding to two equivalent sites (Reaction II with intrinsic constant, 5×10^4 M^{-1}) at finite protein concentrations would give the

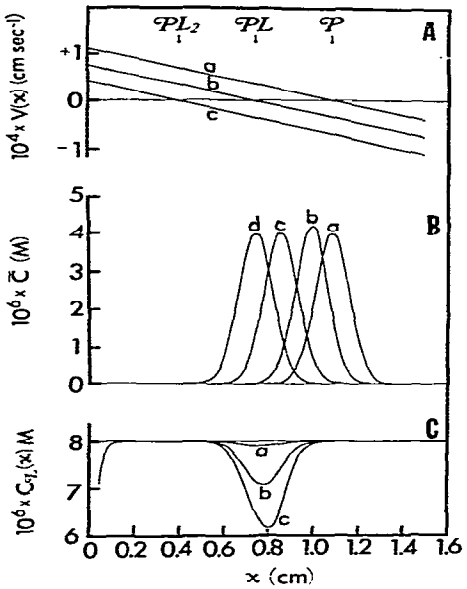

Fig. 3. Theoretical isoelectric focusing patterns (Reaction II with $K_1 = 4 \times 10^5$ M^{-1} and $K_2 = 4 \times 10^4$ M^{-1}). A. Velocity profiles: a, $V_{\mathcal{P}}(x)$; b, $V_{\mathcal{PL}}(x)$; c, $V_{\mathcal{PL}_2}(x)$.
B. Representative focusing patterns illustrating the time-course of approach to the steady-state, $C^0_{\mathcal{P}} = 4 \times 10^{-6}$ M and $C = 8 \times 10^{-6}$ M: a, t=0, b, 4×10^3 s; c, 1.0×10^4 s; d, 1.2×10^5 s. C. Steady-state distribution of free ligand along the isoelectric focusing column, $C = 8 \times 10^{-6}$ M: a, $C^0_{\mathcal{P}} = 4 \times 10^{-6}$ M; b, 4×10^{-5} M; c, 8×10^{-5} M.

same results as reported previously for Reaction I. (Note that eq. (1) is silent with respect to n.) This was found to be so in every respect, thereby lending confidence in the following results for non-statistical binding to two sites.

The representative isoelectric focusing patterns displayed in fig. 3B illustrate the time-course of approach to the steady-state for essentially half-saturating concentration of ligand. Since these particular calculations are for a rather low total protein concentration, $C^0_{\mathcal{P}} = 4 \times 10^{-6}$ M, the peak focuses virtually at the midpoint between $\text{pI}_{\mathcal{P}}$ and $\text{pI}_{\mathcal{PL}_2}$ (i.e., at $\text{pI}_{\mathcal{PL}}$) as distated by the parallel, linear velocity profiles. Moreover, as shown in fig. 4, the plot of log $[(x_f - x_0)/(\bar{x}-x_0) - 1]$ against log C (data points, •) coincides closely with the Sips plot (curve a) and gives $\bar{K}_{app} = 1.25 \times 10^5$ M^{-1} and $\alpha_{app} = 0.755$, which are to be compared with $\bar{K} = 1.26 \times 10^5$ M^{-1} and $\alpha = 0.748$. Such good agreement was realized because, at this low $C^0_{\mathcal{P}}$, the trough

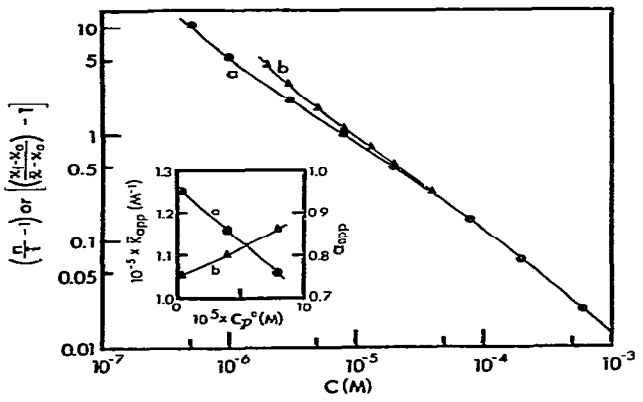

Fig. 4. Sips plot and the analogous plot of theoretical isoelectric focusing data for Reaction II with $K_1 = 4 \times 10^5$ M^{-1} and $K_2 = 4 \times 10^4$ M^{-1}. Curve a, Sips plot of $\log[\bar{r}/\bar{r} - 1]$ against log C (eq. (11)); ●, computer simulated isoelectric focusing data for $C_P^0 = 4 \times 10^{-6}$ M plotted as $\log[(x_f - x_0)/(\bar{x} - x_0) - 1]$ against log C (eq. (12)). Curve b and ▲, simulated focusing data computed for $C_P^0 = 8 \times 10^{-5}$ M and plotted in accordance with eq. (12). The insert shows the extrapolation of $\bar{K}_{app}$ (curve a) and α_{app} (curve b) to infinite dilution of protein.

in the steady-state distribution of free ligand along the column is quite shallow (curve a in fig. 3C). At higher C_P^0 the trough is considerably deeper (fig. 3C) as a consequence of which the log–log plot of the simulated focusing data deviates significantly from the Sips plot; and the higher C_P^0, the greater the deviation. For example, at $C_P^0 = 8 \times 10^{-5}$ M (curve b in fig. 4), $\bar{K}_{app} = 1.06 \times 10^5$ M^{-1} and $\alpha_{app} = 0.861$. It is evident that $\bar{K}_{app}$ and α_{app} must be extrapolated to infinite dilution of protein for accurate determination of $\bar{K}$ and α, as illustrated by the insert to fig. 4.

4. Discussion

Two conclusions can be drawn from the results presented above. First, those for Reaction I generalize the applicability of eq. (1), not only to non-linear velocity gradients, but also to systems where the amount by which each bound ligand molecule increases the velocity of its complex depends upon pH, and non-linearly at that. Evidently, the only critical assumption made in the derivation of eq. (1) is that the velocity profile be linear in the region of the isoelectric point, and this will be approximately so for any continuous function. The perturbing non-linear effects are reflected in the value of the apparent binding constant given by the quotient of the intercept and slope of the linear, double-reciprocal plot of $(\bar{x} - x_0)$ against C; but the results indicate a maximum error of only about 30%. It is important to note, however, that the apparent binding constant must be extrapolated to infinite dilution of protein in order to realize this degree of accuracy.

The second conclusion is that, in principle, isoelectric focusing lends itself to the analysis of the binding of ligand to a population of non-equivalent, non-interacting sites on a protein, as well as statistical binding to equivalent sites. If a Sips distribution of sites is assumed, $\bar{K}$ and α are determined by extrapolation of $\bar{K}_{app}$ and α_{app} to infinite dilution of protein. While the value of $\bar{K}_{app}$ determined at a given protein concentration may be acceptable for some purposes, in general, even a 15% deviation of α_{app} from α will not be, since α is a sensitive measure of the broadness of the distribution. For example, $\alpha = 0.7$ corresponds to a distribution in which 75% of the sites fall in the range $0.16\bar{K}$ to $6\bar{K}$, while for $\alpha = 0.8$ the range is $0.27\bar{K}$ to $3.7\bar{K}$ [8]. Moreover, it is conceivable that under certain experimental conditions α_{app} might approach 1, the value of α for a homogeneous system. Clearly, faithful description of heterogeneous systems depends upon extrapolation to infinite dilution.

Finally, isoelectric focusing data might be interpreted in terms of other models such as a Gaussian distribution of binding energies [4] or a discrete distribution [11], values of the apparent fractional saturation of sites being given by

$$(\bar{r}/n)_{app} = (\bar{x} - x_0)/(x_f - x_0), \qquad (14)$$

which is obtained in a manner analogous to the derivation [1] of eq. (1). In that event, either $(\bar{r}/n)_{app}$ or all of the parameters of the model must be extrapolated to infinite dilution. Analysis of cooperative binding follows that presented herein for binding to heterogeneous sites, the Sips index of heterogeneity in eqs. (9)–(12) being replaced by the Hill coefficient [11].

References

[1] J.R. Cann and K.J. Gardiner, Biophys. Chem. 10 (1979) 211.
[2] L.G. Longworth, Ann. N.Y. Acad. Sci. 41 (1941) 267.

[3] H.A. Abramson, L.S. Moyer and M.H. Gorin, Electrophoresis of proteins and the chemistry of cell surfaces (Reinhold, New York, 1942).
[4] R.N. Pinckard and D.M. Weir, in: Handbook of Experimental Immunology, ed. D.M. Weir (2nd Ed., Blackwell Scientific Publications, Oxford, 1973) ch. 16.
[5] A. Nisonoff, J.E. Hopper and S.B. Spring. The antibody molecule (Academic Press, New York, 1975) ch. 2.
[6] R. Sips, J. Chem. Phys. 16 (1948) 490.
[7] R. Sips, J. Chem. Phys. 18 (1950) 1024.
[8] A. Nisonoff and D. Pressman, J. Immunol. 80 (1958) 417.
[9] A. Nisonoff and D. Pressman, J. Immunol. 81 (1958) 126.
[10] J.R. Cann and D.I. Stimpson, Biophys. Chem. 7 (1977) 103.
[11] F.W. Dahlquist, Methods in Enzymology 48 (1978) 270.